J. Physiol. (1984), **346**, *pp.* 599–619
With 9 text-figures
Printed in Great Britain

ELECTRIC CURRENT FLOW IN A TWO-CELL PREPARATION FROM *CHIRONOMUS* SALIVARY GLANDS

BY P. METZGER AND R. WEINGART

From the Department of Physiology, University of Berne, Bühlplatz 5, CH-3012 Berne, Switzerland

(*Received 20 April 1983*)

SUMMARY

1. Conventional micro-electrode techniques were used to study the passive electrical properties of salivary glands from *Chironomus nuditarsis* insect larvae of the fourth instar stage.

2. Linear cable analysis performed on intact glands revealed the following constants: axial intracellular resistance, $R_i = 2730\ \Omega$ cm; membrane resistance per unit apparent cylindrical area, $R_m = 1350\ \Omega\ cm^2$; membrane capacitance per unit apparent cylindrical area, $C_m = 17{\cdot}6\ \mu F\ cm^{-2}$.

3. The multicellular glands were reduced to intact two-cell preparations by destroying neighbouring cells mechanically. Each cell of a coupled cell pair was impaled with two micro-electrodes, one to pass rectangular current pulses and the other to monitor the resulting voltage deflexions.

4. Internal consistency tests revealed that the experimental data under steady-state conditions may be described accurately by an equivalent circuit consisting of a delta configuration of three resistive elements: the resistances of the non-junctional membrane of cell 1 and cell 2 (r_1 and r_2), and the resistance of the gap junctional membrane connecting the two cells (r_g).

5. The current–voltage relation of the non-junctional membrane was found ohmic over a membrane potential ranging from -40 mV to $+10$ mV. The mean value of R_m was $2020\ \Omega\ cm^2$.

6. The resistance function of the gap junctional membrane was also ohmic. There was no dependence of gap junctional resistance on voltage or direction of current flow, at least over the relatively narrow range of potentials tested ($\sim \pm 10$ mV).

7. Individual values of r_g varied from 20 to 3800 kΩ, with an over-all mean of 1100 kΩ. The lower values are thought to represent the physiological state of cellular coupling, whereas the higher ones may reflect partial uncoupling caused by local damage.

8. The proposed cell pair is a suitable preparation for studying problems related to intercellular coupling.

INTRODUCTION

Salivary glands of *Chironomus* insect larvae have been used extensively to study cell-to-cell coupling (for review, see Loewenstein, 1981). This is due partly to the easy

availability and relatively large cells of the tissue. The merits of this work have been twofold. First, a great deal has been learned about the specific properties of the gap junctions in the insect glandular tissue itself. Secondly, the findings from salivary glands have stimulated similar studies with other types of tissue covering different developmental stages (for references, see Cox, 1974; Bennett, Spray & Harris, 1981; Berkenblit, Boschkowa, Bojzowa, Mittelman, Potapowa, Tschajlachjan & Scharowskaja, 1981; Hertzberg, Lawrence & Gilula, 1981; De Mello, 1982). This has led to the discovery of interesting functional differences between various tissues suggesting the existence of more than one kind of cell-to-cell channel or *connexon*. The outcome is that we now have begun to understand a number of functional aspects of intercellular communication such as the permeability and the effective pore size of a connexion and the ion-controlled regulation of its conductance.

With regard to salivary glands, some features of intercellular coupling remain to be explored. For example, the electrical characterization of the gap junctional membrane remains incomplete. Several investigators have applied linear cable analysis (transmission line analysis) to estimate the electrical resistance of the gap junction (Loewenstein & Kanno, 1964; Loewenstein, Socolar, Higashino, Kanno & Davidson, 1965; Loewenstein, Nakas & Socolar, 1967; Rose, 1971; van Venrooij, Hax, Van Dantzig, Prijs & Denier van der Gon, 1974). The problem with this approach is that, strictly speaking, salivary glands may not fulfil the assumptions underlying classical cable analysis such as uniform cross-sectional diameter, the requirement for parallel current flow, intracellularly and extracellularly, at all distances from the current source (see Hodgkin & Rushton, 1946), or a uniform intracellular and extracellular resistance per unit length. Thus, there is some uncertainty regarding the values calculated for junctional membrane resistance using cable analysis techniques. In addition, this method does not allow further analysis of the electrical properties of the gap junctional membrane other than d.c. resistance. The knowledge of other features such as the voltage dependency of the junctional membrane would obviously be very desirable as well.

This paper utilizes a two-cell preparation which seems conducive to quantitative determinations of the electrical properties of cellular junctions. Functionally coupled cell pairs were obtained by mechanical disruption of neighbouring cells of an intact gland using micro-puncture with a bevelled glass pipette. Each cell of a cell pair was impaled with two conventional micro-electrodes, one to inject current and one to monitor voltage. With this symmetrical arrangement, measurements were taken of the displacements in trans-membrane potential and the applied currents. Quantitative assessments were obtained for both the non-junctional membrane resistance of each individual cell and the gap junctional resistance between the cells. In addition, the voltage dependency was measured for each type of membrane. For comparison, cable analysis was performed using intact glands. This enabled critical evaluation of the limitations inherent to each method, the two-cell and the multicellular approach.

A preliminary report of some of the experiments has been published previously (Metzger & Weingart, 1982).

METHODS

Preparation and solutions

Chironomus nuditarsis larvae (generously supplied by Dr J. Fischer, Department of Zoology, University of Berne) of the fourth instar stage were selected according to the morphologic criteria of Fischer & Rosin (1969). Suitable larvae were immersed in a Petri dish containing experimental medium and decapitated with fine scissors to obtain the salivary glands. The isolated glands were transferred to an experimental chamber with a Pasteur pipette. The bottom of the chamber was coated with a silicon elastomere (Sylgard, Dow-Corning, Seneffe, Belgium) to make the glands gently adhere. The chamber (volume 1 ml) was superfused with physiological saline solution (rate $\geqslant 1$ ml min^{-1}) of the following composition (see also Rose & Rick, 1978) in mM: NaCl, 70; KCl, 4; $CaCl_2$, 4; magnesium succinate, 7; sodium pyruvate, 5; sucrose, 70 (Merck, Darmstadt, F.R.G.); HEPES, 5 (adjusted to pH 7·4 with 1 N-NaOH). All experiments were performed at room temperature (20–22 °C).

A *Chironomus* salivary gland consists of a chain of roughly cylindrical border cells (G cells) circumscribing the lumen of the organ and two sheets of flat cells (F cells) bounding the lumen on the lower and upper side (cf. Rose, 1971). The centre part of the gland was gently touched with a stainless-steel needle to immobilize the organ. According to Rose (1971), this apparently helps to disconnect the F cells from the G cells. A pair of G cells of similar size (100–200 μm in diameter) was selected and the adjacent G cells sequentially destroyed by multiple impalements with a bevelled glass pipette (tip size approximately 2 μm). Success with these manoeuvres rendered the impaired cells opaque and functionally isolated from their neighbours. This was confirmed in preliminary experiments which indicated that current flow was interrupted between intact and opaque cells. The apparent electrical decoupling was presumably mediated by Ca^{2+} leakage into the punctured cell (Oliveira-Castro & Loewenstein, 1971). The above technique resulted in functionally intact two-cell preparations which were viable for several hours during mild experimental interventions.

Signal recording and analysis

Each cell of a coupled cell pair was impaled with two micro-electrodes, one for current passage and the other for recording voltage. Current-passing electrodes were filled with 1·5 M-potassium citrate and voltage-recording electrodes with 3 M-KCl. D.c. tip resistances ranged from 8 to 15 MΩ. The experimental arrangement is illustrated schematically in Fig. 1*A*. Small rectangular current pulses of variable amplitude and either polarity were injected intracellularly and the resulting deflexions of membrane potential measured using the recording electrodes. In this manner, current could be applied independently to each cell. The electrodes were placed in standard Ag/AgCl electrode holders (EH-R, WP-Instruments, Hew Haven, CN, U.S.A.) containing electrode-filling solution and connected to a unity gain electrometer (M 701, WP-Instruments). To pass current, the potassium citrate electrodes were disconnected electrically from the electrometers by a break-away box. The total current flow was measured with a virtual ground circuit connected to the bath via a Ag/AgCl pellet and a 3 M-KCl agar bridge. After pre-amplification, the voltage and current signals were displayed on a four-channel chart recorder (Brush 2400, Gould, Cleveland, OH, U.S.A.).

A simple model of the electrically coupled cell pair was used for analysis of the data (for other models, see Loewenstein *et al.* 1967; Ito, Sato & Loewenstein, 1974). The equivalent circuit is illustrated in Fig. 1*B*. This circuit was described previously by Watanabe & Grundfest (1961) and later generalized by Bennett (1966, 1977). According to this scheme, the current flow in a two-cell preparation can be described using the following lumped resistive elements: r_1 and r_2, the resistances of the non-junctional membrane of cell 1 and cell 2, and r_g, the resistance of the gap junctional membrane connecting the two cells. The model assumes that current flows via either of two pathways: (1) directly through the non-junctional membrane, or (2) through the junctional membrane into the other cell. In addition, the cytoplasmic resistance is lumped with the resistance of the junctional membrane, and the resistance of the extracellular medium is neglected. Capacitative elements were omitted because only the steady-state situation was regarded.

When a constant current pulse (I_1) is injected into cell 1, a membrane potential deflexion will result in both the ipsilateral cell (V_1) and contralateral cell (V_2'). Conversely, injection of constant

current into cell 2 (I_2) will give rise to a voltage deflexion in cell 2 (V_2) and cell 1 (V_1'). Employing Kirchhoff's laws, four equations can be deduced from the equivalent circuit (Watanabe & Grundfest, 1961):

$$\frac{dV_1}{dI_1} = \frac{r_1(r_g+r_2)}{r_1+(r_g+r_2)}, \tag{1}$$

$$\frac{dV_2}{dI_2} = \frac{r_2(r_g+r_1)}{(r_1+r_g)+r_2}, \tag{2}$$

$$\frac{dV_2'}{dI_1} = \frac{r_1 r_2}{r_1+(r_g+r_2)}, \tag{3}$$

$$\frac{dV_1'}{dI_2} = \frac{r_1 r_2}{(r_1+r_g)+r_2}. \tag{4}$$

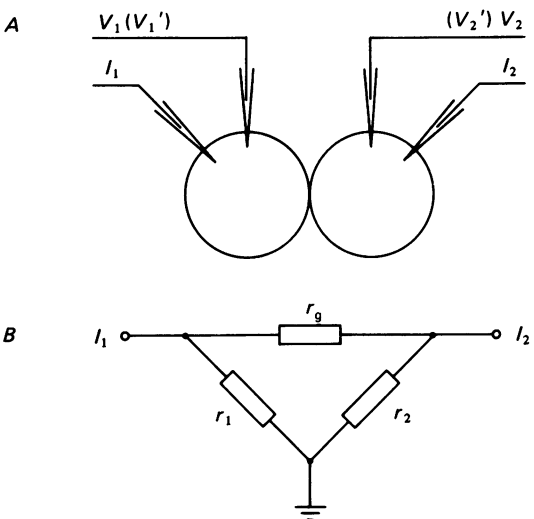

Fig. 1. *A*, experimental arrangement for determining the passive electrical properties of an electrically coupled two-cell preparation. Each of the two cells was impaled with two micro-electrodes, one to pass current (I_1 and I_2) and the other to measure trans-membrane voltage (V_1 and V_1', V_2 and V_2', respectively. *B*, equivalent electric circuit adopted for analysis of resistive elements in the two-cell preparation: r_1 and r_2 represent the non-junctional membrane resistance of cell 1 and cell 2, and r_g the resistance of the gap junctional membrane.

The *input resistance* (eqns. (1) and (2)) is defined as the slope of the voltage–current relation that results from the voltage deflexion arising from the cell to which current is applied. The *transfer resistance* (eqns. (3) and (4)) is defined as the slope of the voltage–current relation that results from the voltage deflexion arising from the contralateral cell to which current is applied. With this set of relationships, four independent measurements can lead to a quantitative evaluation of the three resistive elements described in the equivalent circuit. Since eqns. (3) and (4) express the same combination of resistors, an internal check is included on the consistency of the measurements.

Two special cases result when current is applied simultaneously to both cells that simplify the analysis of the resistive elements. In addition, these measurements test the validity of applying the postulated model. Simultaneous injection of current in both cells (I_1 and I_2) leads to membrane potential displacements in cell 1 (V_1^*) and in cell 2 (V_2^*). If $V_1^* - V_2^* = 0$, the potential difference

across r_g is zero and no net current flows across the gap junction. Therefore, the following relationships hold:

$$\frac{dV_1^*}{dI_1} = r_1, \tag{5}$$

and

$$\frac{dV_2^*}{dI_2} = r_2. \tag{6}$$

The slopes of the voltage–current relations simply determine the resistance of the non-junctional membrane of each individual cell. Another special case can be generated by setting $V_1^* = 0$. This can be achieved by current injection of opposite polarity in cell 1 (I_1) and cell 2 (I_2). Since no potential difference exists across r_1, the total current I_1 is constrained to flow across r_g. Thus, the potential difference across r_g must be identical to V_2^* because both result from the same net current flow. Therefore,

$$\frac{dV_2^*}{dI_1} = r_g, \tag{7}$$

and

$$\frac{dV_2^*}{d(I_1 - I_2)} = r_2. \tag{8}$$

An analogous pair of equations results when $V_2^* = 0$.

RESULTS

Cable analysis in intact salivary glands

Fig. 2 illustrates an experiment in which the passive electrical properties of an intact salivary gland were determined using one-dimensional cable analysis (see, e.g. Weidmann, 1952; Jack, Noble & Tsien, 1975). Constant current pulses were applied at the apex of the gland via a micro-electrode inserted in the cell most distal from the glandular duct. Displacements of membrane potential resulting from current flow were measured with two (in some cases only with one) recording micro-electrodes. One electrode impaled various cells along one branch of the array of G cells. The other electrode was positioned in the same cell as the current-passing electrode. This served to assess the stability of the preparation during the measurements. The electrodes were inserted as close as possible to the centre of the cells and the geometry was measured through the binocular microscope.

Fig. 2*A* shows a plot of the logarithm of the steady-state voltage deflexion *vs.* distance (x) from the current injection site. The data points closely approximated the theoretical curve for an infinite cable, $V = V_0 \exp(-x/\lambda)$, where λ = length constant. In this experiment, the electrical length constant was 579 μm. There was no indication of a deviation from an exponential voltage decay with distance in the vicinity of the current electrode. This finding suggests that no large three-dimensional voltage gradients are present (Eisenberg & Johnson, 1970). Fig. 2*B* shows the geometry of the preparation with the cell lengths drawn to scale. From a comparison of Fig. 2*A* and *B* it is evident that the injected current must have spread over many cell lengths. Fig. 2*A* also shows the plot of the half-time of the rise of the voltage deflexions ($t_{\frac{1}{2}}$) *vs.* distance (x) (Hodgkin & Rushton, 1946; see also Jack *et al.* 1975). The slope of this relationship equals $\tau/2\lambda$. Hence τ, the membrane time constant, for the illustrated experiment was 11·4 ms.

Cable parameters were determined in seven successful experiments. The collected

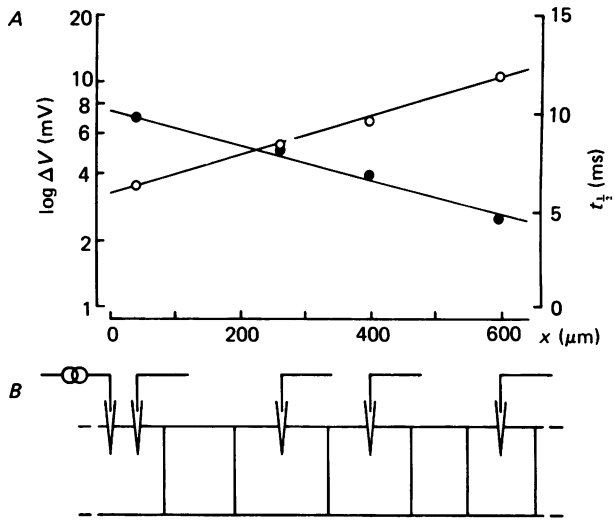

Fig. 2. Linear cable analysis performed on an intact salivary gland. *A*, left ordinate (●): logarithm of steady-state electrotonic response to applied current; abscissa: distance from the current injection site, x. The straight line shows the voltage distribution predicted for an infinite cable (space constant $\lambda = 579$ μm; $r^2 = 0{\cdot}98$). *A*, right ordinate (○): half-time of rise of the voltage deflexions, $t_{\frac{1}{2}}$; abscissa: distance x. The slope of this relationship was 0·008 ms μm^{-1} ($r^2 = 0{\cdot}99$) and equals $\tau/2\lambda$. Thus, τ was 11·6 ms. *B*, geometry of the preparation, represented as a linear array of cylindrical cells drawn to scale. For analysis, the position of the voltage electrode was assumed to be identical with the centre of the cell; preparation M 5.

TABLE 1. Electrical constants obtained from intact salivary glands

Preparation	E_m (mV)	λ (μm)	τ (ms)	R_m (Ω cm²)	R_i (Ω cm)	r_g (kΩ)	C_m (μF cm⁻²)
M 2	−28	449	27	1462	3625	139	18·4
M 4	−21	488	13·7	1010	1697	107	13·5
M 5	−40	579	11·6	1085	1133	119	10·7
M 28	−26	620	33	2416	2200	157	13·6
M 156a	−23	390	17·4	831	2048	126	20·9
M 156d	−24	520	35·4	1197	1771	105	29·6
M 156e	−18	345	23·7	1431	6611	167	16·6
Mean		484	23·1	1347	2726	131	17·6
±S.E. of mean		40	3·8	213	765	10	2·6

The following parameters were measured: the membrane potential (E_m), the input resistance (R_{in}), the length constant (λ), the membrane time constant (τ), the cellular geometry of the preparations and the locations of impalement with the electrodes. The following electrical constants were computed: the specific non-junctional membrane resistance (R_m), the specific inside longitudinal resistance (R_i), the non-specific resistance of the gap junctional membrane (r_g), and the specific capacitance of the non-junctional membrane (C_m).

results are summarized in Table 1. The mean λ was 484 μm, and the mean τ was 23·1 ms. The specific electrical constants were calculated using the values of the input resistance ($R_{in} = 2V_0/I_0$), λ, τ, and the geometry of the preparation (assuming a cylindrical cell chain extending to infinity on both sides of the current electrode). The following values were obtained: axial intracellular resistance, $R_i = 2726 \pm 765$ Ω cm

(mean ± S.E. of the mean); membrane resistance per unit apparent cylindrical area, $R_m = 1347 \pm 213\ \Omega\ cm^2$; membrane capacitance per unit apparent cylindrical area, $C_m = 17{\cdot}6 \pm 2{\cdot}6\ \mu F\ cm^{-2}$. If we assume a specific membrane capacitance of 1 $\mu F\ cm^{-2}$, the membrane resistance per unit membrane area would be $R_m' = 23700\ \Omega\ cm^2$. More convenient for a direct comparison of these data with those to be extracted from the two-cell preparation (see below and Table 2) is the intracellular longitudinal resistance to axial current flow, r_i. Neglecting the contribution of the cytoplasmic resistivity, from the individual values of r_i and the average cell length, the resistance of the gap junctional membrane, r_g was calculated. The average r_g turned out to be $131 \pm 10\ k\Omega$.

Ideally, application of one-dimensional cable analysis to the G-cell layer in salivary glands would require negligible electrical interaction between G cells and F cells. The existence of some contacts between the two types of cells has been inferred from both morphological and functional investigations (Kloetzel & Laufer, 1969; Rose, 1971; Berger & Uhrik, 1972). However, on physiological grounds, the large difference in size between G cells and F cells tends to minimize the contribution of the F cells to the current spread along the G cell layer. This is because the input resistance is inversely related to the diameter of the cellular conduit.

Electrical properties of a two-cell preparation

In the preceding experiments, entire salivary glands were used to determine the passive electrical properties. This approach still leaves uncertainties as to the behaviour of a single cellular junction. Therefore, we reduced the multicellular arrangement to a two-cell preparation to simplify further the analysis.

Current injection into one of the cells. Fig. 3 shows the records from an experiment in which current pulses of 220 ms duration were applied consecutively to either of the cells. During each pulse, three signals were recorded simultaneously: I_1, V_1 and V_2' or I_2, V_2 and V_1'. There was a consistent degree of attenuation of the voltage response when current was applied separately to either side of the junction. This suggested that current spreads across the gap junctional membrane equally well in both directions.

The collected electrotonic responses then were analysed in terms of the equivalent circuit described previously (see Fig. 1). Fig. 4 shows the analysis of the records illustrated in Fig. 3 (filled symbols) and other data (open symbols) from the same experiment. Panels *A* and *B* represent the results from current application into cells 1 and 2 respectively. The slope of the plot of V_1 or V_2 *vs.* total current flow represents the input resistance function of cell 1 and cell 2 (see eqns. (1) and (2), Methods section). In contrast, the slope of the plot of V_1' or V_2' *vs.* current corresponds to the transfer resistance function (see eqns. (3) and (4)).

Very often, the depolarizing range of trans-membrane voltages were explored less completely than the hyperpolarizing ones. This was because of rectification of the current-passing electrodes. Nevertheless, it was clear that the input and transfer resistance functions remained remarkably linear within the voltage range tested. This suggests ohmic resistances of the non-junctional membranes. Furthermore, this also implies constancy of the ratio transfer resistance/input resistance, which represents the attenuation factor for the current flow across a junction. In other words, the gap

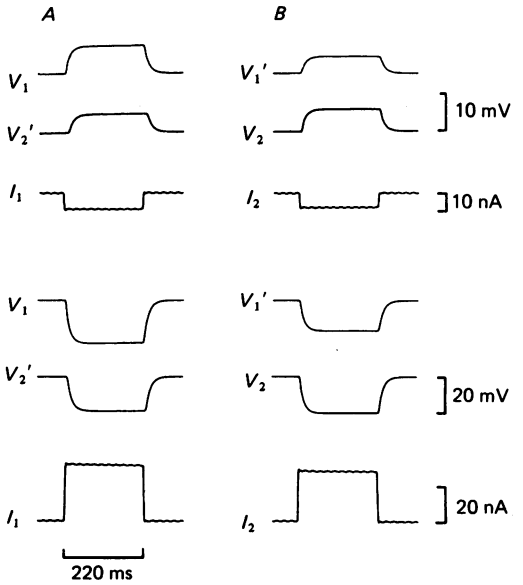

Fig. 3. Electrotonic spread of current in a two-cell preparation. *A*, a small rectangular current pulse of 220 ms duration was injected into cell 1 (I_1) in two directions: membrane depolarizing (upper panel) and membrane hyperpolarizing (lower panel). Traces V_1 and V_2' represent the resulting voltage deflexions in cell 1 and cell 2, respectively. *B*, records of the symmetrical case of current injection into cell 2 (I_2); preparation M 31.

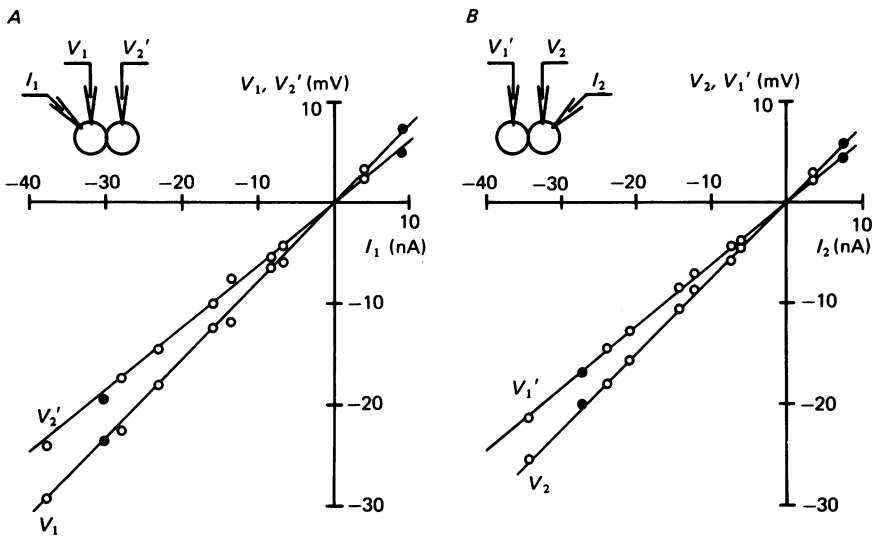

Fig. 4. Voltage–current plots of a complete experiment performed on a two-cell preparation. The inserts show diagrams of the electrode arrangement. The slope of V_1 (or V_2) *vs.* I_1 (or I_2) determines the input resistance function, and the slope of V_2' (or V_1') *vs.* I_1 (or I_2) corresponds to the transfer resistance function. Depolarization is upwards, hyperpolarization downwards. The closed circles show the analysis of the records illustrated in Fig. 3. The straight lines were obtained by linear regression analysis ($r^2 > 0{\cdot}98$ in all cases). *A*, current injection into cell 1. *B*, current injection into cell 2; preparation M 31.

junctional membrane acts as an ohmic resistor within the voltage range tested. As an internal check on the consistency of the measurements, we compared the slopes of the transfer resistance functions. These should be equal since both describe the same combination of the resistive elements in the equivalent circuit. Comparison of Fig. 4*A* and *B* reveals that they can be superimposed. The slopes of the transfer resistance functions, obtained by least-square analysis, were 0·616 mV nA^{-1} and

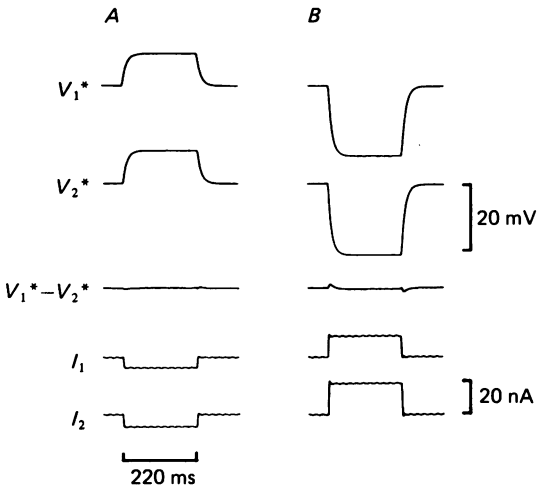

Fig. 5. Simultaneous current application to both sides of the junction. The voltage deflexion in one cell (V_1*) was set by an appropriate current (I_1). The electrotonic potential in the other cell (V_2*) then was adjusted to the same value by manipulating the current in the other cell (I_2) such that $V_1^* - V_2^* = 0$. This experiment was performed using varying intensities of depolarizing (*A*) and hyperpolarizing (*B*) current pulses; preparation M 31.

0·622 mV nA^{-1} for V_1' and V_2', respectively. Taking a mean value of 0·619 mV nA^{-1}, the resistances of the non-junctional membrane of cell 1 and cell 2, r_1 and r_2, and the gap junctional resistance, r_g, the following values were calculated (eqns. (1) and (2)): $r_1 = 1590$ kΩ, $r_2 = 1240$ kΩ, and $r_g = 330$ kΩ.

Simultaneous current injection in both cells. Another test of the validity of the equivalent circuit involves use of eqns. (5) and (6). Rectangular current pulses must be injected simultaneously into both cells such that the voltage deflexions in cell 1 (V_1*) and cell 2 (V_2*) are equal (i.e. $V_1^* - V_2^* = 0$). The voltage–current relations become simpler since the voltage drop across r_g is zero.

Fig. 5 illustrates the pen recorder tracings of such an experiment performed on the same preparation as shown in Figs. 3 and 4. Traces V_1* and V_2* represent the respective voltage deflexions in cells 1 and 2 during simultaneous current injection in both cells. The difference trace $V_1^* - V_2^*$ demonstrates that there was minimal voltage difference across r_g.

The graphical analysis of the records illustrated in Fig. 5 (filled symbols) and other records of the same run (open symbols) are shown in Fig. 6. Panel *A* depicts the voltage–current relationship for r_1, and panel *B* the corresponding one for r_2. The linearity of both graphs suggests that the non-junctional membrane resistance of each

individual cell must be ohmic within this range of voltages. From the slopes r_1 and r_2 were calculated to be 1570 kΩ, and 1210 kΩ respectively. These values are in good agreement with those obtained from the experiment exemplified in Figs. 3 and 4, in which current was injected into only one of the cells.

Current of opposite polarity also was applied in both cells (I_1 and I_2) to force the voltage displacement in cell 1 (V_1*) or cell 2 (V_2*) to be zero. In this case, eqns. (7) and

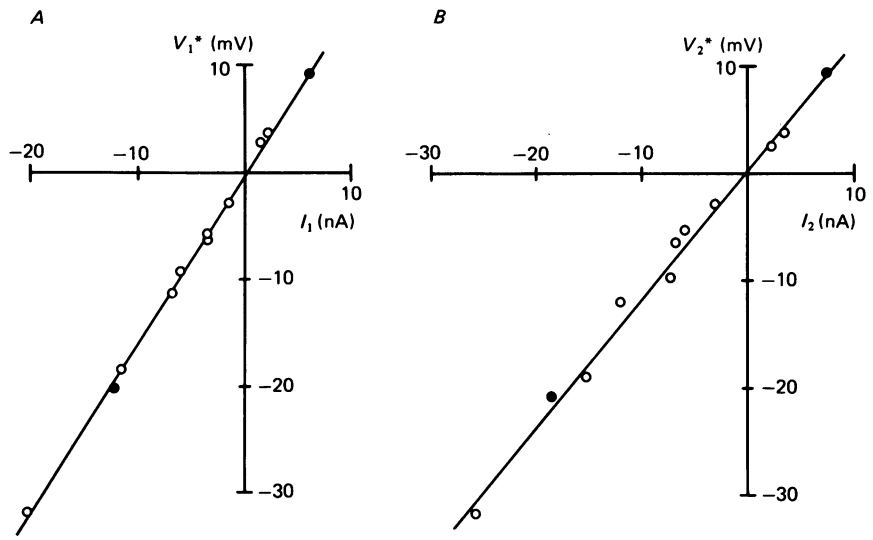

Fig. 6. Voltage–current relationship across r_1 (V_1*/I_1), panel *A*, and r_2 (V_2*/I_2), panel *B*, under the condition of no potential difference across r_g. This condition was achieved by simultaneous current application to both sides of the junction so that V_1* − V_2* = 0. The filled circles correspond to the values extracted from the electrotonic responses exemplified in Fig. 5. The lines were obtained by linear regression analysis and revealed values for r_1 and r_2 of 1570 kΩ ($r^2 > 0{\cdot}99$) and 1210 kΩ ($r^2 > 0{\cdot}99$), respectively; preparation M 31.

(8) are applicable. Unfortunately, this experiment was difficult to perform in some preparations because of a coupling coefficient approximating 1·0 and problems with electrode rectification.

Fig. 7*A* exemplifies a successful experiment of this type. The intensity of the individual current pulses was adjusted such that alternatively V_1* = 0 or V_2* = 0. Subsequently, the current pulse applied to cell 2 was delayed by 400 ms so as to separate the two pulses with respect to time. The resulting signals for current and voltage are illustrated in Fig. 7*B*. This procedure allowed measurement of individual currents (I_1 and I_2) as well as an analysis in terms of the single pulse mode (see *Current injection into one of the cells*). By the use of eqns. (7) and (8) and the data from the experiment presented in Fig. 7*A*, r_1 and r_2 were calculated to be 470 kΩ and 830 kΩ, respectively, and r_g 740 kΩ. From eqns. (1) and (4) and the data generated by delaying the current pulse (Fig. 7*B*), r_1 and r_2 were calculated as 460 kΩ and 610 kΩ, respectively, and r_g as 680 kΩ. The agreement between the different sets of resistance values was remarkably good and suggests that the equivalent circuit (Fig. 1) provides a good approximation of the experimental conditions.

Voltage–current relationship of the gap junction. The voltage–current relationship of the gap junctional membrane was obtained by combining the data illustrated in Figs. 4 and 6. The resulting graphical plot is shown in Fig. 8. It involves pairs of values of voltage drop across r_g and the effective current applied, i.e. V_g and I_g, respectively. Individual values of V_g were obtained from the experiment illustrated in Fig. 4. From

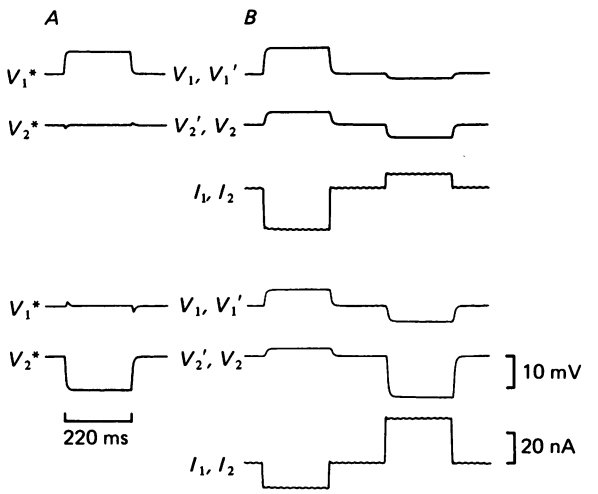

Fig. 7. Comparison between simultaneous and sequential current application to the two-cell preparation. *A*, first, current of opposite polarity was injected simultaneously in both cells such that the resulting voltage deflexion in cell 2 (V_2*, upper panel) or in cell 1 (V_1*, lower panel) remained at 0. *B*, the chosen current pulses were then applied sequentially by introducing a delay of 400 ms between I_1 and I_2. This enabled comparative analysis in terms of the single current injection mode. For nomenclature of electrotonic responses (V_1, V_2', and V_2, V_1'), see legend to Fig. 3; preparation M 33.

the equivalent circuit (Fig. 1*B*) it follows that $V_g = V_1 - V_2'$ or $V_2 - V_1'$, depending upon whether current was applied to cell 1 (Fig. 4*A*) or cell 2 (Fig. 4*B*). The current I_g which produced V_g could not be determined from this experiment. However, it could be estimated from the experiment illustrated in Fig. 6 using the following reasoning. For example, the current intensity which produced V_1* by flowing through r_1 (Fig. 6*A*) must be equivalent to that which caused V_1' by flowing first through r_g and then r_1 (Fig. 4*B*), provided V_1* and V_1' are of identical amplitude. Since r_g and r_1 are in series, V_g and V_1' must have been produced by the same current. An analogous procedure was used to derive I_g from V_2* (Fig. 6*B*) and V_2' (Fig. 4*A*).

The triangles and circles in Fig. 8 represent individual data points resulting from current application to cell 1 and cell 2, respectively. Linear regression analysis revealed slopes of 0·339 mV nA^{-1} (△) and 0·311 mV nA^{-1} (○) for the two cases. Because the slopes were virtually identical all data points were pooled. The combination of data yielded an over-all slope of 0·319 mV nA^{-1} ($r = 0{\cdot}993$, $n = 22$) corresponding to a gap junctional membrane resistance of 319 kΩ. The linear nature and the identical magnitude of the slopes of both functions suggest that the resistance

of the gap junctional membrane is ohmic and does not discriminate as to the direction of current flow.

Compilation of the results from the two-cell experiments. Table 2 summarizes the results from fourteen successful experiments with two-cell preparations. The data is organized according to experimental approach. Method 1 refers to the experiments in which single current pulses were applied to either cell of a preparation. The analysis

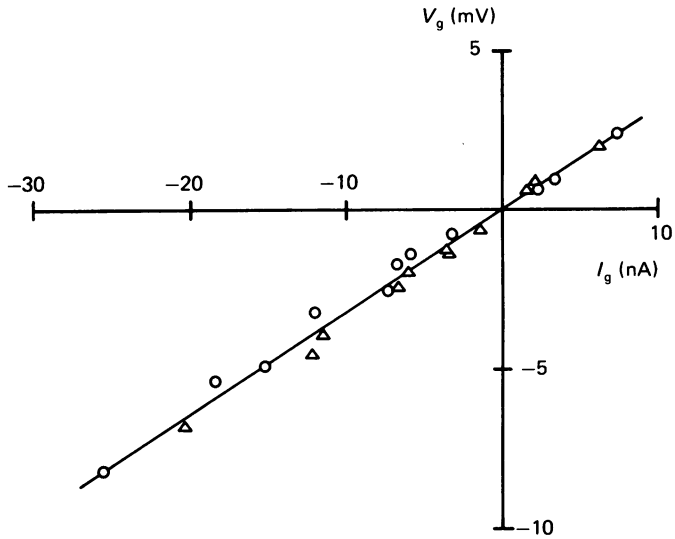

Fig. 8. Voltage–current relation of the gap junctional membrane, derived from the data points plotted in Fig. 6 and the slopes of the input and transfer resistance functions illustrated in Fig. 4. A least-square analysis was performed on the data from current injection into cell 1 (△) and cell 2 (○), revealing a slope of 0·319 mV nA^{-1} ($r^2 = 0{\cdot}98$); preparation M 31.

involved eqns. (1) to (4). The transfer resistance functions (eqns. (3) and (4)) express identical combinations of resistances. Their numerical values agreed to within 16% and thus their average was used for further computations. Simultaneous application of current pulses to both cells of a preparation was achieved in methods 2 and 3. In method 2 the net current forced to flow across the gap junctional membrane was set to 0; analysis was then performed using eqns. (5) and (6). In method 3 the current pulses were chosen such that no voltage deflexions occurred in a given cell; in this case, eqns. (7) and (8) were applied for analysis. Methods 2 and 3 both generated a pair of values for the gap junctional membrane resistance, r_g. Because the individual values of any given pair did not differ by more than 35%, Table 2 gives the average only.

In Table 2 the non-junctional membrane resistances (r_1 and r_2) are expressed in specific terms (R_1 and R_2). This conversion involved the knowledge of the geometry and the size of each cell. At the end of each experiment the cells under investigation were routinely measured by means of a calibrated ocular grid. The calculation of the non-junctional membrane area was accomplished by modelling the over-all shape of the cells by a suitable polyhedron. It involved both the free surface area and the areas

TABLE 2. Electrical constants obtained from two-cell preparations of salivary glands

Preparation	E_m (mV)	Mean coupling coefficient	Method 1 R_1 (Ω cm^2)	Method 1 R_2 (Ω cm^2)	Method 1 r_g (kΩ)	Method 2 R_1 (Ω cm^2)	Method 2 R_2 (Ω cm^2)	Method 2 r_g (kΩ)	Method 3 R_1 (Ω cm^2)	Method 3 R_2 (Ω cm^2)	Method 3 r_g (kΩ)
M 9	−17	0·40	2650	2350	3800	2650	2650	4120			
M 11	−23	0·85	1230	1750	180	1210	1750	250	1220	2170	220
M 13	−25	0·89	3030	4230	440						
M 16	−20	0·65	1960	3240	1600						
M 19	−18	0·52	2680	1830	2800						
M 20	−13	0·50	3000	2390	2560						
M 22a	−15	0·90	2900	4490	460	4080	3230	480			
M 22b	−32	0·95	2200	2900	20						
M 25	−35	0·95	680	1100	50	770	900	50			
M 30	−7	0·77	580	480	160	450	490	150	450	540	170
M 31	−16	0·77	1660	1770	330	1660	1720	320			
M 32	−16	0·73	1500	1710	540	1420	1460	490			
M 33	−17	0·53	650	520	680	650	600	750	660	710	740
M 34	−32	0·44	2000	1140	1750	1320	1150	1710			
Mean		0·70	1910	2135	1100						
±S.E. of mean		0·05	240	330	335						

Three independent experimental approaches were adopted involving current application to either cell of a cell pair (method 1), or simultaneous current application to both cells (methods 2 and 3). Details concerning the experimental arrangement, the choice of the parameters to be measured, and the data analysis are given in the Methods section (p. 601) and the Results section (p. 610). The following constants were computed: the specific non-junctional membrane resistance of each cell (R_1 and R_2, respectively), and the non-specific junctional membrane resistance (r_g).

facing neighbouring cells. No corrections were made for membrane folding. In contrast, the resistances of the gap junctional membrane could not be expressed in specific terms because of the lack of appropriate morphometrical data.

To test for systematic errors in the various experimental methods, the results from the three different methods were compared. A significant correlation was observed between the data of methods 1 and 2, both for the non-junctional and junctional membrane resistances (number of experiments, $n = 9$; R_1, R_2, correlation coefficient, $r = 0{\cdot}90$, test coefficient t distributed, $2\alpha < 0{\cdot}001$; r_g, $r = 0{\cdot}99$, $2\alpha < 0{\cdot}001$). The correlation between the data of methods 1 and 3 was somewhat less significant, presumably because of the small number of experiments ($n = 3$; R_1, R_2, $r = 0{\cdot}975$, $2\alpha < 0{\cdot}1$; r_g, $r = 0{\cdot}999$, $2\alpha < 0{\cdot}01$).

This analysis demonstrates a fairly consistent agreement among the data obtained by the different methods. Therefore, we confined our further analysis to the experimental results obtained from method 1 since the largest number of experiments was performed using this approach. From a total of fourteen experiments the mean values for the non-junctional membrane resistances, R_1 and R_2, were 1910 Ω cm² and 2135 Ω cm², respectively. Statistical analysis revealed that the two means were not significantly different from each other (paired t test: $P > 0{\cdot}5$). The over-all mean of the non-junctional membrane resistance was 2020 Ω cm². The mean value for the junctional membrane resistance, r_g, was found to be 1100 kΩ. Individual values of r_g varied considerably in that they ranged from 20 to 3800 kΩ. This variability is responsible for the rather large standard error of ±335 kΩ.

The second column in Table 2 lists the mean trans-membrane potential E_m. This differed less than 1 mV between the pair of cells. No definite correlation could be established between non-junctional membrane resistance and E_m. This is in accord with the previous finding that the current–voltage relationship of the non-junctional membranes is linear over a relatively large range of membrane potentials (see e.g. Figs. 4 and 6). In addition, no correlation was found between r_g and E_m.

Table 2, third column, gives the mean coupling coefficient of each cell pair. It is defined as the ratio of the voltage deflexion induced in the follower cell divided by the voltage deflexion elicited in the injected cell (V_2'/V_1 and V_1'/V_2, respectively). Individual values varied from 0·4 to 0·95 with an average of 0·7. Many investigators have used this parameter as a measure of the degree of intercellular coupling. For this reason Fig. 9 illustrates the relationship between the junctional membrane resistance r_g and the coupling coefficient. The data points appear to show a non-linear relation which is well approximated by the equation coupling coefficient $= R_{1,2}/r_g + R_{1,2}$. The curve was constructed using the mean value of the experimentally determined resistance of the non-junctional membrane ($R_{1,2} = 2020$ Ω cm²). The progressive steepening of the curve with declining values of the coupling coefficient reflects the growing contribution of a constant non-junctional membrane resistance to the coupling coefficient. In other words, the lower the coupling coefficient, the larger is the underestimate of the real r_g. This kind of reasoning may be important when changes in the intercellular coupling are considered. Furthermore, the apparent non-linear relation between the coupling coefficient and r_g should lend caution to direct inferences from changes in 'coupling' to changes in r_g.

Uncoupled cell pairs

In some preparations spontaneous decoupling developed progressively over 20 to 30 min. This was presumably caused by local damage incurred during the course of either cell preparation and/or impalement (see p. 616). Unequivocally, the coupling coefficient was observed to decrease to values as low as 0·1. Assuming that the input resistance function of the decoupled cell pair corresponds to the input resistance of a single cell, we may use measurements from such preparations to make another estimate of the specific electrical properties of the non-junctional membrane. From five preparations the following parameters were determined: membrane time constant $\tau = 9{\cdot}6 \pm 3{\cdot}2$ ms, specific membrane resistance $R_m = 1070 \pm 300\ \Omega\ cm^2$, specific membrane capacitance $C_m = 8{\cdot}85 \pm 1{\cdot}3\ \mu F\ cm^{-2}$ (means ± S.E. of the mean).

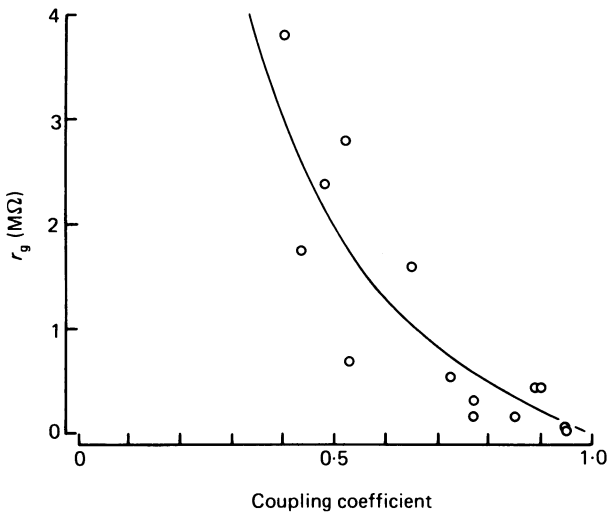

Fig. 9. Comparison between two different parameters used to express intercellular communication; the resistance of the gap junctional membrane, r_g, and the coupling coefficient. The open circles represent the data obtained from method 1 (see Table 1). The smooth curve reflects the relationship between the two parameters (coupling coefficient = $r_{1,2}/(r_g + r_{1,2})$), with $r_{1,2}$ = 2020 kΩ (mean value from determinations under consideration).

DISCUSSION

Non-junctional membrane

Originally, the specific membrane resistance of glandular cells was estimated as 20 to 30 Ω cm² (Lundberg, 1957; Schanne & Coraboeuf, 1966). These rather low values were based on the assumption that exocrine glands were composed of individual cells. A significant advance was made with the discovery of electrical coupling in epithelia (Loewenstein & Kanno, 1964). Since then intercellular coupling has been established as the cause of low input resistances (ranging from 1 to 10 MΩ) in salivary glands of insect larvae and imagines (Loewenstein *et al.* 1967; Kislow & Veprintsev, 1971; Rose, 1971; Ginsborg, House & Silinsky, 1974; van Venrooij *et al.* 1974; Berridge,

Lindley & Prince, 1975), molluscs (Klevets & Shuba, 1974; Kater, Rued & Murphy, 1978) and mammals (Kagayama & Nishiyama, 1974; Nishiyama & Petersen, 1974; Hammer & Sheridan, 1978; Kater & Galvin, 1978; Gallacher & Petersen, 1980).

The extent of the evaluation is limited in the case of a qualitative experimental approach (one double-barrelled micro-electrode, or two separate electrodes impaled in different cells). However, with a more powerful method, e.g. cable analysis (see, e.g. Jack *et al.* 1975), it has been possible to determine the specific resistance of the non-junctional membrane, R_m. At first glance, the published values of R_m for salivary glands seem to vary substantially. This may be illusory since the largest values, namely 9000 to 12000 Ω cm^2 (Loewenstein & Kanno, 1964; Loewenstein *et al.* 1965; Loewenstein *et al.* 1967) include a correction factor for membrane folding. Our mean R_m of 1490 Ω cm^2 corresponds better to the lower values reported by van Venrooij *et al.* (1974), Klevets & Shuba (1974) and Kislov & Veprintsev (1971) of 800 Ω cm^2, 1090 Ω cm^2, and 2290 Ω cm^2, respectively. The question is whether or not the inclusion of a correction factor for membrane folding more closely approximates the true specific membrane resistance. The folding factor of 30 (Wiener, Spiro & Loewenstein, 1964) used by Loewenstein's group may represent an over-estimate. For comparison, in the tissue with the most extensive known membrane folding, the small intestinal epithelium, microvilli increase the apical cell membrane by a factor of 20–30 (see Bloom & Fawcett, 1975; Weiss & Greep, 1977). Without this correction, an upper limit of 400 Ω cm^2 would result from the electrical measurement by Loewenstein's group. Because of the sparsity of morphometrical data it seems reasonable to neglect such corrections for the moment and regard the resulting membrane resistance values as lower limits.

So far the discussion has focused on data gathered from intact tissues. Alternatively, measurements of R_m may also be performed on single cells. In insect salivary glands it has been demonstrated that the syncytial structure disappears prior to pupation and cells functionally isolate from each other (Vozhkova, Kovalev, Mittelman & Shilianskaia, 1970; Kislov & Veprintsev, 1971). Kislov & Veprintsev (1971) have used this ontogenetic phenomenon to their advantage. Working on *Drosophila funebris*, they found a R_m of 1100 Ω cm^2 for such 'single cells'. However, this R_m value may not be identical to that of larval cells since R_m is likely to change with the developmental stage. Our own measurements on decoupled cell pairs lead to an R_m of 1070 Ω cm^2. Since in these preparations decoupling may have been caused by Ca^{2+} entry into the cells (see p. 616), it is conceivable that R_m was reduced by the effect of elevated internal Ca^{2+} concentration on non-junctional membrane conductance. Certainly, Ca^{2+}-injection experiments in gland cells (Loewenstein, 1975; Petersen & Iwatsuki, 1978) provide a precedent for this explanation. Another possibility would be to use single cells isolated by enzymatic treatment (Mangos, 1979; Quissell & Redman, 1979) but to date such electrophysiological investigations have not been performed. Our experiments on intact two-cell preparations revealed an R_m of 2020 Ω cm^2. This value is twice that reported for single cells, presumably for the reasons noted above. It is also slightly larger than most of the values determined from insect glands. Some arguments regarding the discrepancy in reported R_m values are presented below (see p. 616).

There have been few reports about the current–voltage relation of the non-junctional

membrane. An ohmic behaviour over a large range of membrane potentials was found in whole salivary glands of insects (Loewenstein & Kanno, 1964) and mouse (Nishiyama & Petersen, 1974). Nevertheless, these observations do not exclude a degree of rectification of the membrane which might be masked by the cable behaviour (Noble, 1962). However, our own measurements on cell pairs are not hampered by such uncertainties. They clearly demonstrate a linear relationship over a voltage range of 50 mV. This contrasts with the R_m in mouse parotid gland (Gallacher & Petersen, 1980) and snail salivary gland (Klevets & Shuba, 1974) which is distinctly non-ohmic. This non-linearity is expected in view of the spontaneous membrane depolarizations (Gallacher & Petersen, 1980) and action potentials (Hadley, Murphy & Kater, 1980) that have been observed in these cells.

There also are few reports about the specific capacitance (C_m) of the non-junctional membrane. Klevets & Shuba (1974) found a value of 3·5 μF cm^{-2} in intact glands, whereas Kislov & Veprintsev (1971) reported 9·18 μF cm^{-2} for single cells. In comparison, our measurements were 13·5 μF cm^{-2} for intact salivary glands, and 8·85 μF cm^{-2} for single cells of uncoupled cell pairs. Assuming a unit cell membrane with a capacitance of 1 μF cm^{-2} leads to an estimate of the effective non-junctional membrane area and the folding factor. Stereological examination of the cellular envelope will determine whether this reasoning is correct.

Gap junctional membrane

Intercellular communication in salivary glands has been documented both by morphologists (see, e.g. Satir & Gilula, 1973) and physiologists (see e.g. Loewenstein, 1981). Combined studies indicate that the gap junction represents the putative site of interaction between neighbouring cells (Kater & Galvin, 1978; Shimono, Yamamura & Fumagalli, 1980; Maxwell, 1981). Electrical coupling has been established both by intrinsic and elicited potentials. In glands in which non-junctional membranes demonstrates non-linear behaviour, cell-to-cell transmission of spontaneous membrane fluctuations and of action potentials has been observed (Kater *et al.* 1978; Kater & Galvin, 1978). In glands with linear non-junctional membranes, intracellular current application has demonstrated intercellular current flow. At first glance, the coupling coefficient may serve as a convenient index of cell-to-cell coupling. Values ranging from 0·79 to 0·96 were measured in insects (Loewenstein & Kanno, 1964; Loewenstein *et al.* 1965; Vozhkova *et al.* 1970), 0·9 in molluscs (Kater *et al.* 1978) and 0·69 to almost 1 in mammals (Hammer & Sheridan, 1978; Kater & Galvin, 1978). Our own studies on cell pairs revealed a mean value of 0·7 (range, 0·4–0·95).

The intracellular longitudinal resistance (r_i) is a more quantitative parameter for intercellular coupling. It is assumed to represent the series combination of two resistive elements, the cytoplasmic resistance (r_c), and the gap junctional membrane resistance (r_g) ($r_i = r_c + nr_g$; n = number of cells cm^{-1}). For our purposes, r_c will be neglected as a separate entity and be lumped together with r_g. After conversion of some of the published data, the following values of r_g were gathered from the literature: 26 kΩ (Loewenstein & Kanno, 1964; *Drosophila flavorepleta*; calculated from $R_i = 145\ \Omega$ cm^{-1}, and the cross-sectional area of $3{\cdot}5 \times 10^{-5}$ cm^2 (Wiener *et al.* 1964, fig. 2)), 89–190 kΩ (Loewenstein *et al.* 1967; *Chironomus thummi*), 54 kΩ (Rose, 1971; *Chironomus thummi*) and 230–270 kΩ (van Venrooij *et al.* 1974; *Drosophila*

hydei). From our cable analysis on intact glands we obtained an r_g of 125 kΩ which corresponds to previous *Chironomus* data. However, our two-cell experiments yield a mean value for r_g of 1100 kΩ. This rather large value is the result of averaging all cell pairs, even those whose cell-to-cell contact may have been impaired. It is conceivable that our manoeuvres with the glands, e.g. trimming to size, or impalement with four micro-electrodes, may have been responsible for local damage with subsequent entry of Ca^{2+} from the extracellular space. As a consequence, the cells may have become partially decoupled (see, e.g. Oliveira-Castro & Loewenstein, 1971; Rose & Loewenstein, 1976). Therefore, we tend to believe that our lowest values of r_g are more representative of the physiological state of intercellular coupling. If we limit ourselves to the four experiments where the coupling coefficient was highest (M 11, M 22b, M 25 and M 30 of Table 1), r_g takes a value of the order of 100 kΩ. Unfortunately, no stereological parameters are available at present concerning the gap junctional membrane of salivary glands. This information would be necessary to express the values of r_g in specific terms and hence important for a comparison with other syncytial tissues.

Our measurements on cell pairs have enabled investigation of the current–voltage relation of the gap junctional membrane. This was found to be linear, at least over the relatively narrow range of voltage tested ($\sim \pm 10$ mV). Future experiments with different methods will be necessary to further test this conclusion over a broader range of potentials. Similar observations were reported previously for the lateral giant axon of crayfish (Watanabe & Grundfest, 1961) and more recently for cardiac tissue of guinea-pig (Kameyama, 1983). However, Spray, Harris & Bennett (1981) have described a voltage-dependent resistance of the junctional membrane in amphibian embryos. To date this is the sole report of this kind but at the same time it is the most thorough one.

We found no sign of rectification of the gap junctional membrane in our studies. This agrees with previous reports by Loewenstein & Kanno (1964) for salivary glands from *Drosophila*, and by Kater & Galvin (1978) on mouse submaxillary glands. In fact, with few exceptions, e.g. the giant motor synapse of crayfish (Furshpan & Potter, 1959), gap junctions show bidirectional transmission of electric signals (for references, see Loewenstein, 1981).

Limitations of the methods

The application of linear cable analysis is based on several assumptions (see Hodgkin & Rushton, 1946): (1) the preparation geometry should resemble a uniform right circular cylinder in structure, (2) the inner core should be small and the membrane resistance high enough that current flow is parallel intra- and extracellularly. For *Chironomus* salivary glands, eliminating the F cells certainly improves the linearity of the array of G cells. However, the G cells are by no means cylindrical nor necessarily in the axis of current flow. They show a polyhedral geometry of cell diameter and length with a low ratio of space constant to cell length. Because of the shape of an individual cell, the preparation resembles a string of pearls with a non-uniform cross section along its length. The decline in cross section towards the points of cell-to-cell contact leads to a decrease in space constant, thus to an over-estimate of r_i and hence of r_g. Furthermore, a considerable amount of non-

junctional membrane is located in the plane of intercellular contacts, which is oriented perpendicular to the axis of current flow. The neglect of this contribution may be of considerable importance. It tends to underestimate R_m and to over-estimate r_g and C_m. The results extracted from experiments performed on intact tissue *vs.* cell pairs (compare Table 1 and 2) agree with these predictions. The discrepancy between the results obtained by the two different methods may also be explained by three-dimensional voltage gradients around a point source of current (Eisenberg & Johnson, 1970). This is because an associated deviation from linear cable behaviour would tend to over-estimate the input resistance of the two-cell preparation. Even though our cable analysis did not provide supporting evidence, we cannot exclude the possibility of at least a small contribution of this kind.

The analysis of the two-cell experiments was based on the assumption of a simple equivalent circuit consisting of three resistors in a delta configuration (see Fig. 1*B*). The validity of this circuit was verified by performing independent types of measurements. Table 2 indicates that the three methods used give similar results. This suggests that the chosen model accurately describes the circuit for steady-state current flow between two cells. This conclusion is further substantiated by the finding that r_g obtained with method 1 was unaffected by the direction of the current flow across the gap junctional membrane.

The cell-pair approach also has some inherent limitations. A practical problem is the damage which may be introduced either by eliminating neighbouring cells and/or by impaling with four micro-electrodes. As already discussed above (see p. 616), manoeuvres which lead to Ca^{2+} leakage into the cytoplasm cause partial uncoupling between cells. Therefore, it may well be that the larger values of r_g were the results of such secondary events. The cell-pair approach has a theoretical limitation as well. The closer the coupling coefficient approaches to unity, the larger the error in determining r_g. The coupling coefficient equals the ratio transfer resistance/input resistance. Thus, the coupling coefficient is maximized when transfer and input resistance are similar in magnitude. This occurs when the voltage deflexions are comparable in size in both cells such that the signal/noise ratio becomes limiting. In other words, the expected error is largest in a tightly coupled preparation. However, in practice the coupling coefficient did not exceed 0·95 (see Table 2, second column) and thus did not create serious problems in this tissue.

In conclusion, we suggest that cell pairs of *Chironomus* salivary glands represent a suitable preparation for investigating problems related to intercellular coupling. For example, they may be particularly appropriate for injection studies since chemical non-homogeneities, unlike in intact gland work, do not affect quantitative analyses.

This paper was submitted to the Faculty of Medicine, University of Berne, in partial fulfilment of a M.D. degree (P.M.). We are grateful to Miss M. Herrenschwand, Messrs C. Cigada and A. Meyer for their expert technical assistance, to Dr Clara Mathys for translating the Slavic literature, and to Professor S. Weidmann and Dr M. Pressler for critical comments. The work was financially supported by the Swiss National Science Foundation (grant 3.565-0.79).

REFERENCES

BENNETT, M. V. L. (1966). Physiology of electrotonic junctions. *Ann. N.Y. Acad. Sci.* **137**, 509–539.

BENNETT, M. V. L. (1977). Electrical transmission: a functional analysis and comparison with chemical transmission. In *Cellular Biology of Neurons*, vol. 1, sect. 1, *Handbook of Physiology, The Nervous System*, ed. KANDEL, E., pp. 357–416. Baltimore: Williams & Wilkins.

BENNETT, M. V. L., SPRAY, D. C. & HARRIS, A. L. (1981). Electrical coupling in development. *Am. J. Zool.* **21**, 413–427.

BERGER, W. K. & UHRIK, B. (1972). Membrane junctions between salivary gland cells of Chironomus thummi. *Z. Zellforsch.* **127**, 116–126.

BERKENBLIT, M. B., BOSCHKOWA, W. P., BOJZOWA, L. J., MITTELMAN, L. A., POTAPOWA, T. W., TSCHAJLACHJAN, L. M. & SCHAROWSKAJA, J. J. (1981). *High Conductance Junctional Membranes* (Russian). Moscow: 'Nauka'.

BERRIDGE, M. J., LINDLEY, B. D. & PRINCE, W. T. (1975). Membrane permeability changes during stimulation of isolated salivary glands of calliphora by 5-hydroxytryptamine. *J. Physiol.* **244**, 549–567.

BLOOM, W. & FAWCETT, D. W. (1975). *A Textbook of Histology*, p. 659. Philadelphia: Saunders.

COX, R. P. (1974). *Cell Communication*. New York: John Wiley & Sons.

DE MELLO, W. C. (1982). Cell-to-cell communication in heart and other tissues. *Prog. Biophys. molec. Biol.* **39**, 147–182.

EISENBERG, R. S. & JOHNSON, E. A. (1970). Three-dimensional electrical field problems in physiology. *Prog. Biophys. molec. Biol.* **20**, 1–65.

FISCHER, J. & ROSIN, S. (1969). Das larvale Wachstum von Chironomus nuditarsis str. *Revue Suisse Zool.* **76**, 727–734.

FURSHPAN, E. J. & POTTER, D. D. (1959). Transmission at the giant motor synapses of the crayfish. *J. Physiol.* **145**, 289–325.

GALLACHER, D. V. & PETERSEN, O. H. (1980). Electrophysiology of mouse parotid acini: effects of electrical field stimulation and ionophoresis of neurotransmitters. *J. Physiol.* **305**, 43–57.

GINSBORG, B. L., HOUSE, C. R. & SILINSKY, E. M. (1974). Conductance changes associated with the secretory potential in the cockroach salivary gland. *J. Physiol.* **236**, 723–731.

HADLEY, R. D., MURPHY, A. D. & KATER, S. B. (1980). Ionic basis of resting and action potentials in salivary gland acinar cells of the snail helisoma. *J. exp. Biol.* **84**, 213–225.

HAMMER, M. G. & SHERIDAN, J. D. (1978). Electrical coupling and dye transfer between acinar cells in rat salivary glands. *J. Physiol.* **275**, 495–505.

HERTZBERG, E. L., LAWRENCE, T. S. & GILULA, N. B. (1981). Gap junctional communication. *A. Rev. Physiol.* **43**, 479–491.

HODGKIN, A. L. & RUSHTON, W. A. H. (1946). The electrical constants of a crustacean nerve fibre. *Proc. R. Soc.* B **133**, 444–479.

ITO, S., SATO, E. & LOEWENSTEIN, W. R. (1974). Studies on the formation of a permeable cell membrane junction. II. Evolving junctional conductance and junctional insulation. *J. Membrane Biol.* **19**, 339–355.

JACK, J. J. B., NOBLE, D. & TSIEN, R. W. (1975). *Electrical Current Flow in Excitable Cells*. Oxford: Clarendon Press.

KAGAYAMA, M. & NISHIYAMA, A. (1974). Membrane potential and input resistance in acinar cells from cat and rabbit submaxillary glands *in vivo*: effects of autonomic nerve stimulation. *J. Physiol.* **242**, 157–172.

KAMEYAMA, M. (1983). Electrical coupling between ventricular paired cells isolated from guinea-pig heart. *J. Physiol.* **336**, 345–357.

KATER, S. B. & GALVIN, N. J. (1978). Physiological and morphological evidence for coupling in mouse salivary gland acinar cells. *J. Cell Biol.* **79**, 20–26.

KATER, S. B., RUED, J. R. & MURPHY, A. D. (1978). Propagation of action potentials through electrotonic junctions in the salivary glands of the pulmonate mollusc, Helisoma trivolvis. *J. exp. Biol.* **72**, 77–90.

KISLOV, A. N. & VEPRINTSEV, B. N. (1971). Electric characteristics of the cellular and nuclear membranes of the salivary gland cells of Drosophila funebris larvae. *Comp. Biochem. Physiol.* **39A**, 521–529.

KLEVETS, M. J. & SHUBA, M. F. (1974). Electrical characteristics of plasma membranes from salivary gland cells of Helix pomatia (Ukrainian). *Fiziol. Zh. SSSR* **20**, 540–542.

KLOETZEL, J. A. & LAUFER, H. (1969). A fine-structure analysis of larval salivary gland function in Chironomus thummi. *J. Ultrastruct. Res.* **29**, 15–36.

LOEWENSTEIN, W. R. (1975). Permeable junctions. *Cold Spring Harb. Symp. quant. Biol.* **40**, 49–63.

LOEWENSTEIN, W. R. (1981). Junctional intercellular communication: The cell-to-cell membrane channel. *Physiol. Rev.* **61**, 829–913.

LOEWENSTEIN, W. R. & KANNO, Y. (1964). Studies on an epithelial (gland) cell junction. 1. Modifications of surface membrane permeability. *J. Cell Biol.* **22**, 565–586.

LOEWENSTEIN, W. R., NAKAS, M. & SOCOLAR, S. J. (1967). Junctional membrane uncoupling. Permeability transformations at a cell membrane junction. *J. gen. Physiol.* **50**, 1865–1891.

LOEWENSTEIN, W. R., SOCOLAR, S. J., HIGASHINO, S., KANNO, Y. & DAVIDSON, N. (1965). Intercellular communication: renal, urinary bladder, sensory, and salivary gland cells. *Science, N.Y.* **149**, 295–298.

LUNDBERG, A. (1957). The mechanism of establishment of secretory potentials in sublingual gland cells. *Acta physiol. scand.* **40**, 35–58.

MANGOS, J. A. (1979). Morphological and functional characterization of isolated human parotid acinar cells. *J. dent. Res.* **58**, 2028–2035.

MAXWELL, D. J. (1981). The presence of gap junctions in the septate desmosomes of the salivary apparatus of the cockroach nauphoeta cinerea. *J. exp. Biol.* **94**, 341–344.

METZGER, P. & WEINGART, R. (1982). Passive electrical properties of insect salivary gland cells. *Experientia* **38**, 716.

NISHIYAMA, A. & PETERSEN, O. H. (1974). Membrane potential and resistance measurement in acinar cells from salivary glands *in vitro*: effect of acetylcholine. *J. Physiol.* **242**, 173–188.

NOBLE, D. (1962). The voltage dependence of the cardiac membrane conductance. *Biophys. J.* **2**, 381–393.

OLIVEIRA-CASTRO, G. M. & LOEWENSTEIN, W. R. (1971). Junctional membrane permeability. Effect of divalent cations. *J. Membrane Biol.* **5**, 51–77.

PETERSEN, O. H. & IWATSUKI, N. (1978). The role of calcium in pancreatic acinar cell stimulation-secretion coupling: an electrophysiological approach. *Ann. N.Y. Acad. Sci.* **307**, 599–618.

QUISSELL, D. O. & REDMAN, R. S. (1979). Functional characteristics of dispersed rat submandibular cells. *Proc. natn Acad. Sci. U.S.A.* **76**, 2789–2793.

ROSE, B. (1971). Intercellular communication and some structural aspects of membrane junctions in a simple cell system. *J. Membrane Biol.* **5**, 1–19.

ROSE, B. & LOEWENSTEIN, W. R. (1976). Permeability of a cell junction and the local cytoplasmic free ionized calcium concentration. *J. Membrane Biol.* **28**, 87–119.

ROSE, B. & RICK, R. (1978). Intracellular pH, intracellular free Ca, and junctional cell–cell coupling. *J. Membrane Biol.* **44**, 377–415.

SATIR, P. & GILULA, N. B. (1973). The fine structure of membranes and intercellular communication in insects. *A. Rev. Ent.* **18**, 143–166.

SCHANNE, O. & CORABOEUF, E. (1966). Potential and resistance measurements of rat liver cell in situ. *Nature, Lond.* **210**, 1390–1391.

SHIMONO, M., YAMAMURA, T. & FUMAGALLI, G. (1980). Intercellular junctions in salivary glands. Freeze fracture and tracer studies of normal rat sublingual gland. *J. Ultrastruct. Res.* **72**, 286–299.

SPRAY, D. C., HARRIS, A. L. & BENNETT, M. V. L. (1981). Equilibrium properties of a voltage-dependent junctional conductance. *J. gen. Physiol.* **77**, 95–117.

VAN VENROOIJ, G. E. P. M., HAX, W. M. A., VAN DANTZIG, G. F., PRIJS, V. & DENIER VAN DER GON, J. J. (1974). Model approaches for the evaluation of electrical cell coupling in the salivary gland of the larva of Drosophila hydei. The influence of lysolecithin on the electrical coupling. *J. Membrane Biol.* **19**, 229–252.

VOZHKOVA, V. P., KOVALEV, S. A., MITTELMAN, L. A. & SHILIANSKAIA, E. N. (1970). Changes in the conductivity of intercellular contacts in the process of cell differentiation in the salivary gland of the Drosophila virilis larvae at the 3rd stage of development (Russian). *Tsitologiia* **12**, 1108–1115.

WATANABE, A. & GRUNDFEST, H. (1961). Impulse propagation at the septal and commissural junctions of crayfish lateral giant axons. *J. gen. Physiol.* **45**, 267–308.

WEIDMANN, S. (1952). The electrical constants of Purkinje fibres. *J. Physiol.* **118**, 348–360.

WEISS, L. & GREEP, R. O. (1977). *Histology*, pp. 679–681. New York: McGraw-Hill.

WIENER, J., SPIRO, D. & LOEWENSTEIN, W. R. (1964). Studies on an epithelial (gland) cell junction. II. Surface structure. *J. Cell Biol.* **22**, 587–598.